Free Radical Biology and Medicine 91 (2016) 58–67

Contents lists available at ScienceDirect

Free Radical Biology and Medicine

journal homepage: www.elsevier.com/locate/freeradbiomed

Original Contribution

MicroRNA-2861 regulates programmed necrosis in cardiomyocyte by impairing adenine nucleotide translocase 1 expression

Kun Wang [a,*,1], Bo Long [b,1], Na Li [c,1], Ling Li [c], Cui-Yun Liu [a], Yan-Han Dong [a], Jin-Ning Gao [a], Lu-Yu Zhou [a], Chao-Qun Wang [a], Pei-Feng Li [a,*]

[a] Center for Developmental Cardiology, Institute for Translational Medicine, College of Medicine, Qingdao University, Qingdao 266021, China
[b] Laboratory of Molecular Medicine, Central Research Laboratory, Peking Union Medical College Hospital, Chinese Academy of Medical Sciences and Peking Union Medical College, Beijing 100730, China
[c] State Key Laboratory of Biomembrane and Membrane Biotechnology, Institute of Zoology, Chinese Academy of Sciences, Beijing 100101, China

ARTICLE INFO

Article history:
Received 2 October 2015
Received in revised form
22 November 2015
Accepted 27 November 2015
Available online 30 November 2015

ABSTRACT

Necrosis is programmed and is one of the main forms of cell death in the pathological process in cardiac diseases. MicroRNAs (miRNAs) have emerged as key gene regulators in many diseases. However, how miRNAs contribute to programmed necrosis is poorly defined. Here we report that miR-2861 and adenine nucleotide translocase 1 (ANT1) constitute an axis that regulates necrotic cell death in the heart. Our results show that ANT1 inhibits H_2O_2-induced cardiomyocytes necrosis. ANT1 also antagonizes myocardial necrosis in a mouse ischemia/reperfusion (I/R) model. We further demonstrate that miR-2861 directly binds to the coding sequence of ANT1 and suppresses the expression of ANT1 mRNA and protein. MiR-2861 induces necrotic cell death. In contrast, knockdown of miR-2861 attenuates H_2O_2-induced necrosis in cardiomyocytes. Also, miR-2861 knockdown protects heart from I/R injury and necrotic cell death in vivo. MiR-2861 regulates necrosis and myocardial infarction through targeting ANT1. Collectively, these data identify miR-2861 and ANT1 as two novel regulators of cardiomyocyte necrosis and myocardial infarction, and suggest potential therapeutic targets in treatment of cardiac diseases.

1. Introduction

Heart failure is a lethal disease with a worse life expectancy than many other diseases. Many studies revealed that cardiomyocyte death played an important role in heart failure [1,2]. Hitherto, necrosis is responsible for cardiomyocyte death during myocardial infarction and heart failure [3,4]. Studying the mechanism of necrosis in cardiomyocyte would be of great importance for tackling heart diseases.

Adenine nucleotide translocator 1 (ANT1), also called ADP/ATP translocase 1, is a multi-pass membrane protein that locates in the mitochondrion inner membrane [5]. The mouse *Ant1* genes are very similar in sequence to its human homologs [6]. ANT1 facilitates the exchange of cytosolic ADP and mitochondrial ATP across the mitochondrial inner membrane [7]. ANT proteins form channels that exchange ATP and ADP and control the levels of ATP in the cytoplasm [8]. ANT plays an essential role in cellular energy metabolism and provide a continuous supply of ADP to mitochondria [9,10]. Although ANT1 is specifically expressed in heart tissues, the function mechanism of ANT1 in the progression of cardiomyocyte necrosis remains unknown [11].

MiRNAs are small non-coding RNA molecules, about 21–25 nucleotides in length [12,13]. Growing evidences have demonstrated that miRNAs play a significant role in the regulation of various biological functions [14–17]. MiRNAs also participate in the regulation of cardiovascular diseases [18–20]. In particular, miRNAs are involved in the pathogenesis of cardiac diseases such as myocardial infarction and heart failure, and manipulation of miRNAs can be developed to therapeutic approaches [18,21,22]. However, whether and how miRNAs participate in the signal pathway that regulates necrosis in the heart remains unknown.

Our present work aims at finding out molecules and signaling pathway that are able to regulate cardiomyocyte necrosis. Our report for the first time reveals that ANT1 inhibits cardiomyocyte necrosis and myocardial infarction. MiR-2861 is found to participate in the regulation of cardiomyocyte necrosis by targeting ANT1. MiR-2861 regulates ANT1 levels by binding to the coding region of ANT1 and triggering ANT1 mRNA degradation. Our results reveal a novel programmed necrosis regulating model which is composed of miR-2861 and ANT1.

* Corresponding authors.
E-mail addresses: wangk696@163.com (K. Wang), peifengliqd@163.com (P.-F. Li).
[1] These authors contributed equally to this work.

http://dx.doi.org/10.1016/j.freeradbiomed.2015.11.031
0891-5849/

2. Methods

2.1. Cardiomyocytes culture and treatment

Cardiomyocytes were isolated from 1 to 2 days old mice as we described [23]. Cells were treated with 150 μM or 700 μM H_2O_2 for cell death assay.

2.2. Cell death assays

Cell death was measured by Alexa Fluor® 488 annexin V/Dead Cell Apoptosis Kit. All PI positive cells (PI+) were indicated as necrotic cells, while Annexin V positive/PI negative cells (Annexin V+/PI−) were considered as apoptotic cells. Necrotic cell death was assessed by lactate dehydrogenase (LDH) activity according to the manufacturer's instruction.

2.3. Cell transfection with miR-2861 mimics or antagomirs

The miR-2861 mimics were synthesized by GenePharma Co.Ltd. MiR-2861 mimic sequence was 5′-GGGGCCUGGCGGCGGGCGG-3′. Mimic control sequence was 5′-UUCUCCGAACGUGUCACGUTT-3′. Chemically modified antisense oligonucleotides (antagomirs) were used to inhibit endogenous miR-2861 expression. The antagomir sequence was 5′-CCGCCCGCCGCCAGGCCCC-3′. The antagomir control sequence was 5′-CAGUACUUUUGUGUAGUACAA-3′. All the bases were 2′-O-methyl-modified (GenePharma Co. Ltd). Cells were transfected with miRNA mimics (50 nM) or antagomirs (50 nM) using Lipofectamine 2000 (Invitrogen) according to the manufacturer's instructions.

2.4. Target protector preparation and transfection

Target protector was designed and named as others and we described [24], In brief, ANT1-$TP^{miR\text{-}2861}$ sequence is 5′-GGGGTCTGGCAGCATCCCCTTGGCA-3′, $TP^{control}$ sequence is 5′-TGACAAATGAGACTCTCTCCTCTCC-3′. They were synthesized by Gene Tools, and transfected into the cells using the Endo-Porter kit (Gene Tools) according to the kit's instructions.

2.5. Quantitative reverse transcription-polymerase chain reaction (qRT-PCR)

Stem-loop qRT-PCR for mature miR-2861 was performed as described [25] on a CFX96 Real-Time PCR Detection System (Bio-Rad). Total RNA was extracted using Trizol reagent. After DNAse I (Takara, Japan) treatment, RNA was reverse transcribed with reverse transcriptase (ReverTra Ace, Toyobo). The levels of miR-2861 analyzed by qRT-PCR were normalized to that of U6. U6 primers were forward: 5′-GCTTCGGCAGCACATATACTAA-3′; reverse: 5′-AACGCTTCACGAATTTGCGT-3′. qRT-PCR for ANT1 were performed as we described [23]. The sequences of ANT1 primers were forward: 5′-GCAGTACAAAGGCATCATTGAT-3′; reverse: 5′- AAGGCGAAGTTCAGGGCTTGA-3′. The results were standardized to control values of glyceraldehyde-3-phosphate dehydrogenase (GAPDH). GAPDH forward primer: 5′-TGTGTCCGTCGTGGATCTGA-3′; reverse: 5′-CCTGCTTCACCACCTTCTTGA-3′. The specificity of the PCR amplification was confirmed by agarose gel electrophoresis.

2.6. Immunoblot

Immunoblot was performed as we described [26]. Briefly, the cells were lysed for 1 h at 4 °C in a lysis buffer (20 mmol/L Tris pH 7.5, 2 mmol/L EDTA, 3 mmol/L EGTA, 2 mmol/L dithiothreitol (DTT), 250 mmol/L sucrose, 0.1 mmol/L phenylmethylsulfonyl fluoride, 1% Triton X-100) containing a protease inhibitor cocktail. The samples were subjected to 12% SDS-PAGE and transferred to nitrocellulose membranes. Equal protein loading was controlled by Ponceau Red staining of membranes. Blots were probed using the primary antibodies. The anti-ANT1 and anti-Actin were from Abcam. After four times washing with PBS, the horseradish peroxidase-conjugated secondary antibodies were added. Antigen–antibody complexes were visualized by enhanced chemiluminescence.

2.7. Measurement of ATP and mitochondrial complex activities

ATP levels were measured using a luciferase-based ATP determination kit (Molecular Probes). In brief, cardiomyocytes were washed with PBS, and then covered with lysis buffer. Samples were centrifuged and the supernatant was retrieved for use in the ATP assay according to the manufacturer's instructions. Luciferase activity was measured by using a luminometer. Complex II and IV enzyme activities of isolated mitochondria were detected using Microplate assay kits (Mitosciences) according to the manufacturer's instructions.

2.8. ANT1 expression constructs

ANT1 adenoviral constructs were prepared using the Adeno-X™ Expression System (Clontech, Mountain View, CA, USA) according to the manufacturer's instructions. In brief, ANT1 was synthesized by PCR using mouse cDNA as the template. The forward primer was 5′-ATGGGGGATCAGGCTTTGAGCTTT-3′; the reverse primer was 5′-TTACACATATTTTTTGATCTC-3′. The PCR fragment was finally cloned into the Adeno-X vector. All constructs were amplified in HEK293 cells. Adenoviral infection of cardiomyocytes was performed as we described [27].

2.9. RNA interference (RNAi)

The mouse ANT1 RNAi target sequence is 5′- GCAGATCTTCCTGGGAGGC-3′. A nonrelated, scrambled RNAi without any other match in the mouse genomic sequence was used as a control (5′- GCTCGAGACTGGCAGTCGT-3′). The adenoviruses harboring these RNAi constructs were generated using the pSilencer™ adeno 1.0-CMV System (Ambion, Grand Island, NY, USA) according to the Kit's instructions. Adenoviruses were amplified in HEK-293 cells.

2.10. Preparations of the luciferase construct of ANT1 CDS and luciferase activity assay

ANT1 CDS was amplified by PCR. The forward primer was 5′-ATGGGGGATCAGGCTTTGAGCTTT-3′; the reverse primer was 5′-TTACACATATTTTTTGATCTC-3′. The constructs were sequence verified. CDS were subcloned into the pGL3 vector (Promega) immediately downstream of the stop codon of the luciferase gene. The introduction of mutations in the putative miR-2861 binding site was performed with the QuikChange II XL Site-Directed Mutagenesis Kit (Stratagene) using the wild type vector as a template. The construct was sequenced to check that only the desired mutations had been introduced. Luciferase activity assay was performed using the Dual-Luciferase Reporter Assay System (Promega) according to the manufacturer's instructions.

2.11. Animal experiment

Male adult C57BL/6 mice (10–12 weeks old) were obtained from Institute of Laboratory Animal Science of Chinese Academy of Medical Sciences (Beijing, China). For delivery of miR-2861 antagomirs, the mice received on three consecutive days, intravenous injections of miR-2861 antagomirs, or its control at a

dose of 35 mg/kg body weight in a small volume (0.2 ml) per injection. For intracoronary delivery of adenoviruses, the mice were anesthetized and ventilated with a HX-300S animal ventilator. The chest was entered through a small left anterior thoracotomy, the pericardial sac was then removed, and 2×10^{11} moi adenoviruses of ANT1 were injected with a catheter from the apex of the left ventricle into the aortic root while the aorta and pulmonary arteries were cross-clamped. The clamp was maintained for 20 s when the heart pumped against a closed system. After removal of air and blood, the chest was then closed and the mice were returned back to cage for recovery. Five days after the injection of adenoviruses, the mice were subjected to I/R surgery. For ANT1 target protectors delivery, the target protectors were delivered to the mice by i.v. injection once daily for 3 consecutive days at 25 mg/kg and the mice were then subjected to I/R surgery.

For I/R injury model, mice were subjected to 60 min ischemia, then 24 h or 1 week reperfusion as described [28]. Sham-operated group experienced the same procedure except the snare was left untied. Evans blue dye was treated as described [28], the areas of infarction (INF), area at risk (AAR), and nonischemic left ventricle (LV) were assessed with computer-assisted planimetry (NIH Image 1.57) by an observer blinded to the sample identity. The ratio of INF/LV were calculated as described [28]. All experiments were performed according to the protocols approved by the QingDao University Animal Care Committee.

2.12. Echocardiographic assessment

Transthoracic echocardiographic analysis was performed on mice after the sham or I/R surgery as we described [24]. Echocardiographic parameters were measured. Fractional shortening (FS) of left ventricular diameter was calculated as [(LVIDd–LVIDs)/LVIDd] × 100. After in vivo evaluation of cardiac function the mice were euthanized and the hearts were harvested, weighted and used for histological examination.

2.13. Statistical analysis

Data are expressed as the mean ± SEM of at least three independent experiments. The differences among experimental groups were evaluated by one-way ANOVA analysis of variance. A value of $p < 0.05$ was considered significant.

3. Results

3.1. H_2O_2 and I/R induce a decrease in the levels of ANT1 expression

We tested the effect of H_2O_2 on cardiomyocyte death and observed that treatment with 150 μM H_2O_2 only triggered apoptosis, while the concentration of 700 μM H_2O_2 preferentially caused necrosis (Fig. 1A and B). We detected the expression of ANT1 in cardiomyoyctes treated with 700 μM H_2O_2. Noticeably, ANT1 mRNA levels (Fig. 1C) and protein levels (Fig. 1D) were dramatically reduced in response to H_2O_2 treatment. To understand the pathophysiological role of ANT1, we tested whether ANT1 is involved in the pathogenesis of myocardial infarction in the animal model. Our results showed that ANT1 expression levels were also markedly decreased upon ischemia/reperfusion (I/R) injury (Fig. 1E and F). These data suggest that ANT1 is involved in H_2O_2- and I/R-induced necrotic cell death.

3.2. ANT1 inhibits necrotic cell death in cardiomyocytes and in the heart

Subsequently, we tested whether ANT1 plays a functional role in cardiomyocyte necrosis and observed that enforced expression of ANT1 (Supplementary Fig. 1A) attenuated necrotic cell death induced by H_2O_2, as assessed by PI exclusion (Fig. 2A and B) and LDH release assay (Fig. 2C). Thus, these results indicate that ANT1 inhibits H_2O_2-induced necrotic cell death.

Mouse model of ischemia/reperfusion (I/R) is widely used for the study of myocardial infarction and I/R has been documented to induce necrosis in the heart. We further investigated the role of ANT1 in the pathogenesis of myocardial infarction in the animal model. Myosin antibody injection technique was used to assess myocardial necrosis. Our results showed that I/R caused a massive increase in necrotic myosin-positive cells, whereas the administration of ANT1 (Supplementary Fig. 1B) resulted in a decrease in the myocardial necrosis (Fig. 2D). The administration of ANT1 also reduced myocardial infarct sizes (Fig. 2E). Echocardiography on animals revealed that ANT1-administrated mice displayed a decrease in left ventricular internal diameter (Fig. 2F) and an amelioration in cardiac function, as indicated by increased fractional shortening (Fig. 2G). Taken together, our results strongly suggest a possible contribution of ANT1 in inhibiting necrosis in I/R injured heart.

3.3. miR-2861 participates in the regulation of ANT1 expression

MiRNA is able to suppress gene expression. To explore the underlying mechanism by which ANT1 is downregulated upon H_2O_2 and I/R treatment, we tested whether miRNA can control ANT1 expression. We analyzed the 3′-untranslated region (UTR) sequence of ANT1 and no potential miRNA binding sites were found. We analyzed the coding sequence (CDS) of ANT1 and observed a region that is complementary to miR-2861 (Fig. 3A). We then attempted to evaluate if miR-2861 modulated ANT1 expression. miR-2861 levels were significantly upregulated in response to 700 μM H_2O_2 treatment in cardiomyocytes (Fig. 3B). Enforced expression of miR-2861 (Supplementary Fig. 2A) resulted in an obvious reduction of ANT1 mRNA and protein levels (Fig. 3C). In contrast, knockdown of miR-2861 (Supplementary Fig. 2B) resulted in an increase in ANT1 mRNA and protein levels (Fig. 3 D). Knockdown of miR-2861 also attenuated the decrease in ANT1 mRNA and protein levels upon H_2O_2 treatment (Fig. 3 E). Thus, it seems that miR-2861 can specifically regulate ANT1 expression.

To understand whether miR-2861 directly target ANT1 coding sequence, we cloned ANT1 coding sequence containing miR-2861 binding site downstream of the luciferase reporter gene (ANT1-CDS-wt). miR-2861 induced a decrease in the luciferase activity (Fig. 3F). The introduction of mutations (ANT1-CDS-mut) in the miR-2861 binding site of ANT1 CDS (Supplementary Fig. 3A) substantially reduced the inhibitory effect of miR-2861 (Fig. 3 F). In addition, we also cloned ANT1 3′UTR and employed the luciferase assay to test whether miR-2861 influenced the translation of ANT1. The luciferase reporter assay revealed that miR-2861 has no effect on the luciferase activity (Fig. 3G). Taken together, it suggests that ANT1 is a specific target of miR-2861.

3.4. miR-2861 regulates H_2O_2-induced cardiomyocyte necrosis

Next, we explored the role of miR-2861 in necrotic regulation. Enforced expression of miR-2861 induced cardiomyocytes necrosis, as assessed by PI exclusion (Fig. 4A) and LDH release assay (Fig. 4B). However, knockdown of endogenous miR-2861 attenuates H_2O_2-induced necrosis in cardiomyocytes (Fig. 4 C and D). These data suggest that miR-2861 plays a fundamental role in H_2O_2-induced cardiomyocyte necrosis.

3.5. miR-2861 regulates necrotic cell death in the heart

We further detected the role of miR-2861 in the pathogenesis of

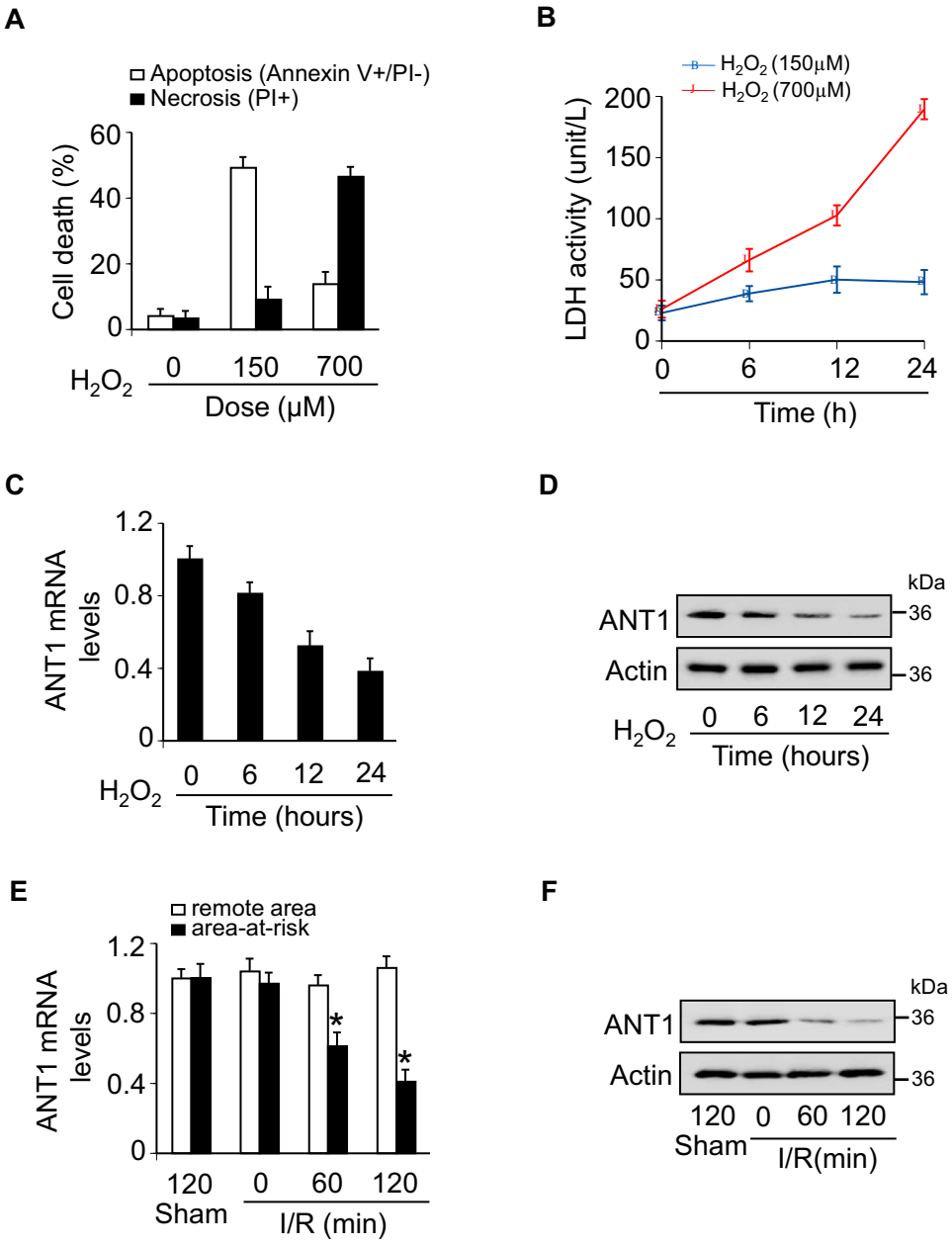

Fig. 1. ANT1 expression is decreased in response to H_2O_2 or I/R treatment. (A) Apoptotic and necrotic cells were analyzed by flow cytometry using Annexin V/PI assay in cardiomyocytes treated with H_2O_2 at the indicated concentration for 24 hours. Necrosis, PI+; Apoptosis, Annexin V+/PI−. (B) LDH activity was measured. Cardiomyocytes were exposed to 150 μM H_2O_2 or 700 μM H_2O_2 at the indicated time ($n=3$). (C and D) ANT1 mRNA and protein levels were detected by qRT-PCR (C) and immunoblot (D) in cardiomyocytes treated with 700 μM H_2O_2 at the indicated time. (E and F) Mice were subjected to cardiac I/R at the indicated time. Sham-operated group served as negative control. Ischemic zone and Remote zone were prepared at the indicated time for qRT-PCR analysis of ANT1 mRNA levels (E). *$p < 0.05$ vs 0 min or sham. (F) The blots showed the representative protein levels of ANT1.

myocardial infarction in the animal model. We observed that miR-2861 levels were elevated in response to I/R injury (Fig. 5A). miR-2861 antigomir (anta-2861) or antigomir control (anta-NC) were injected into mice to knockdown endogenous miR-2861 expression level in the heart. The administration of miR-2861 antagomir resulted in an increase in ANT1 expression (Supplementary Fig. 3B) and a reduction in the myocardial necrosis (Fig. 5B and C). Myocardial infarct size was also attenuated in the anta-2861 group (Fig. 5D) and the cardiac function was ameliorated by knockdown of miR-2861 (Fig. 5E and F). Thus, miR-2861 may have a significant role in the regulation of myocardial necrosis.

3.6. *miR-2861 regulates necrosis through targeting ANT1*

We then explored how miR-2861 exerts its effect on necrotic program. As miR-2861 suppresses ANT1 expression, we thus tests whether ANT1 is a downstream mediator of miR-2861. Knockdown of miR-2861 inhibited the decrease of ANT1 expression and necrotic cell death induced by H_2O_2 treatment. However, the inhibitory effect of miR-2861 knockdown was attenuated by knockdown of ANT1 (Fig. 6A and B). To further confirm the relationship between miR-2861 and ANT1 in necrosis program machinery, we employed the target protector technology in which a target protector is able to disrupt the specific interaction of miRNA–mRNA pairs. To this end, we produced ANT1 target protector

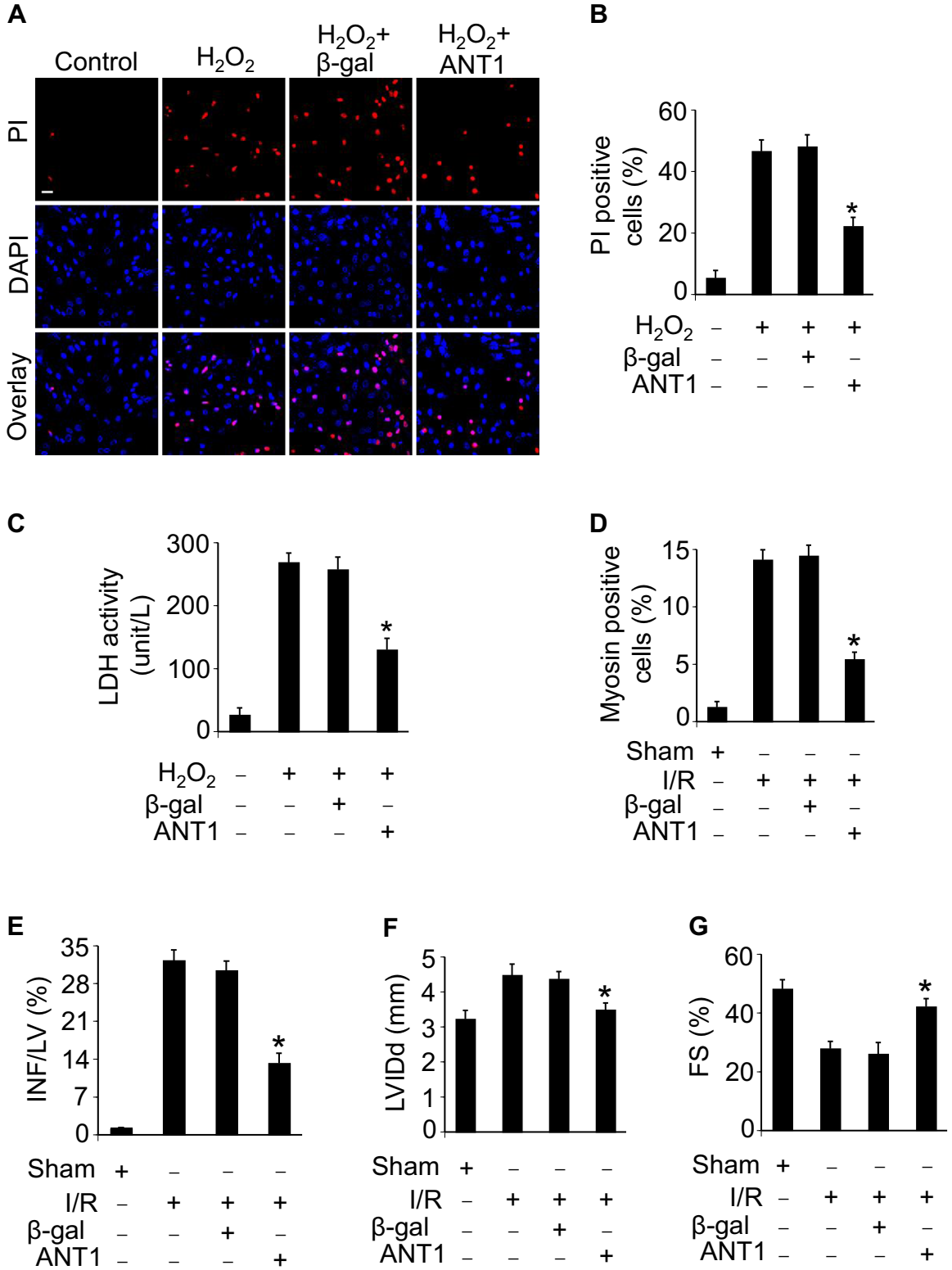

Fig. 2. ANT1 regulates necrotic cell death in cardiomyocytes and in the heart. (A and B) ANT1 reduces necrotic responses induced by H_2O_2. Cardiomyocytes were infected with adenoviral ANT1 or β-gal. 24 h after infection cells were treated with 700 μM H_2O_2. Necrotic cell death was assessed by PI assay. Representative images showed PI-positive cells (A). Red, PI positive nuclei; Blue, DAPI stained nuclei. Bar=20 μm. The quantitative analysis of necrosis was shown in (B). $^*p<0.05$ vs H_2O_2 alone. (C) Cardiomyocytes were treated as described in (A), LDH activity was measured. $^*p<0.05$ vs H_2O_2 alone. (D) ANT1 attenuates myocardial necrosis upon I/R treatment. Mice were subjected to I/R as described in methods. Percentage of cells with myosin antibody infiltration was shown. $n=6$, $^*p<0.05$ vs I/R alone. (E) Enforced expression of ANT1 attenuates myocardial infarction sizes. Mice were treated as described in (D). Myocardial infarct sizes were measured as described in Methods. Left ventricle (LV), infarct area (INF) ($n=6$). $^*p<0.05$ vs WT+I/R. (F and G) Left ventricular dimensions and cardiac function in mice exposed to I/R were analyzed. Mice were treated as described in (D). Transthoracic echocardiographic analysis was performed after 60 min ischemia followed by 1 week reperfusion. LVIDd, diastolic left ventricular internal diameters; FS, fractional shortening of left ventricular diameter, calculated as [(LVIDd–LVIDs)/LVIDd] × 100. ($n=6$). $^*p<0.05$ vs WT+I/R. (For interpretation of the references to color in this figure legend, the reader is referred to the web version of this article.)

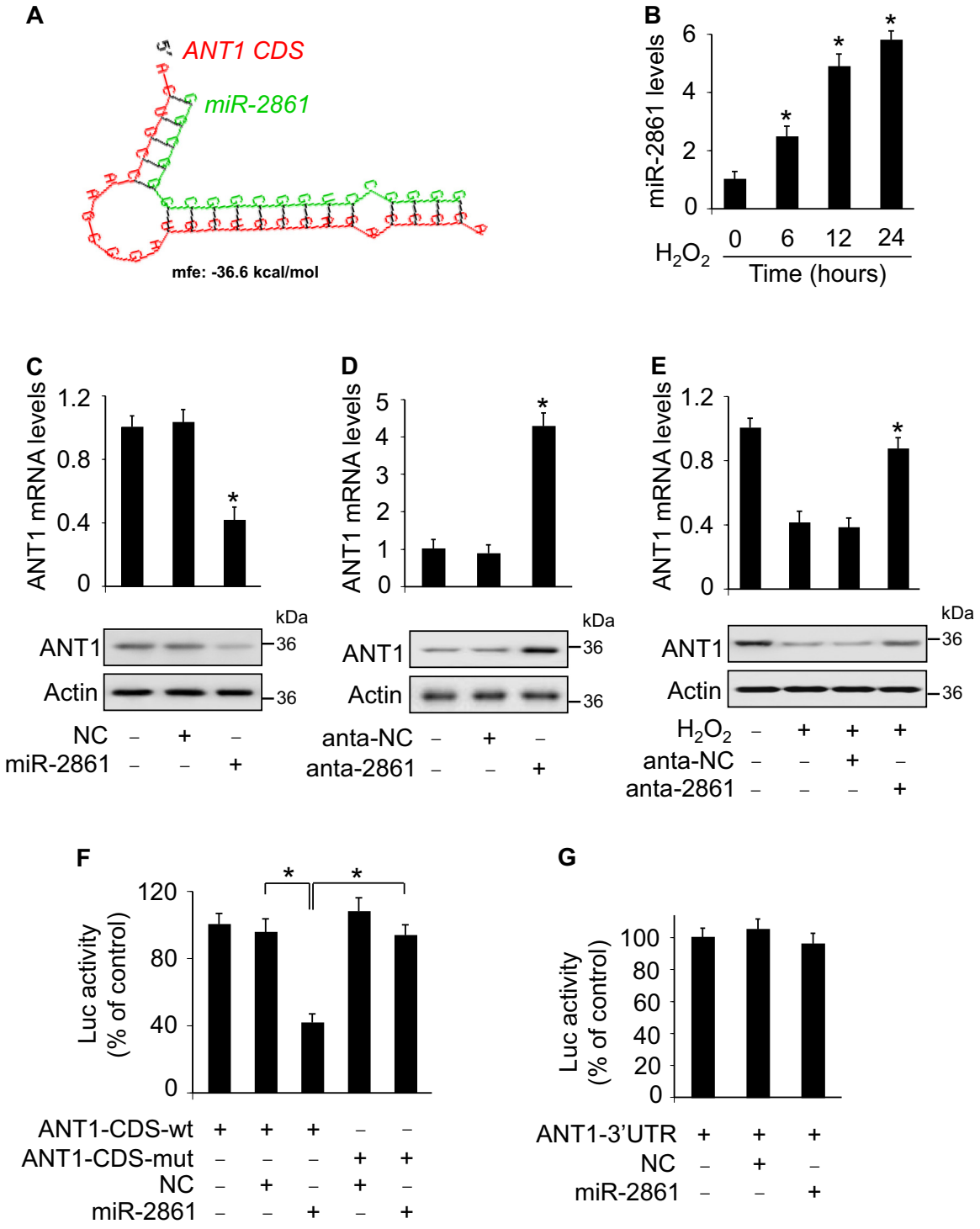

Fig. 3. miR-2861 participates in the regulation of ANT1 expression. (A) Putative miR-2861 site in the coding sequence (CDS) of ANT1. This putative miR-2861 site in the ANT1 CDS was analyzed by RNAhybrid program. (B) Cardiomyocytes were treated with H_2O_2 at the indicated time, and the expression of miR-2861 was analyzed. $^*p < 0.05$ vs control. (C) ANT1 mRNA and protein levels were detected in cardiomyocytes transfected with mimic miR-2861 or mimic control (NC). $^*p < 0.05$ vs control. (D) The mRNA and protein levels of ANT1 were detected in cardiomyocytes transfected with antagomir-2861 (anta-2861) or antagomir control (anta-NC). $^*p < 0.05$ vs control. (E) Cardiomyocytes were transfected with anta-2861 or anta-NC. 24 h after transfection cells were treated with H_2O_2. The mRNA and protein levels of ANT1 were detected. $^*p < 0.05$ vs H_2O_2 alone. (F) Luciferase assay. HEK293 cells were transfected with miR-2861 or NC, then transfected with the luciferase constructs of the wild-type ANT1 coding sequence (ANT1-CDS-wt) or a mutated ANT1 coding sequence (ANT1-CDS-mut). The luciferase activity was analyzed. $^*p < 0.05$. (G) Luciferase assay. HEK293 cells were transfected with miR-2861 or NC, then transfected with the luciferase constructs of the ANT1 3′UTR region (ANT1-3′UTR). The luciferase activity was analyzed.

and observed that ANT1 expression was increased in the presence of ANT1 target protector upon H_2O_2 treatment (Fig. 6C). ANT1 target protector also protected cardiomyocytes from H_2O_2-induced necrotic cell death (Fig. 6D). In the animal model, the target protector of ANT1 resulted in the increase of ANT1 mRNA levels (Supplementary Fig. 4A) and protein levels (Supplementary

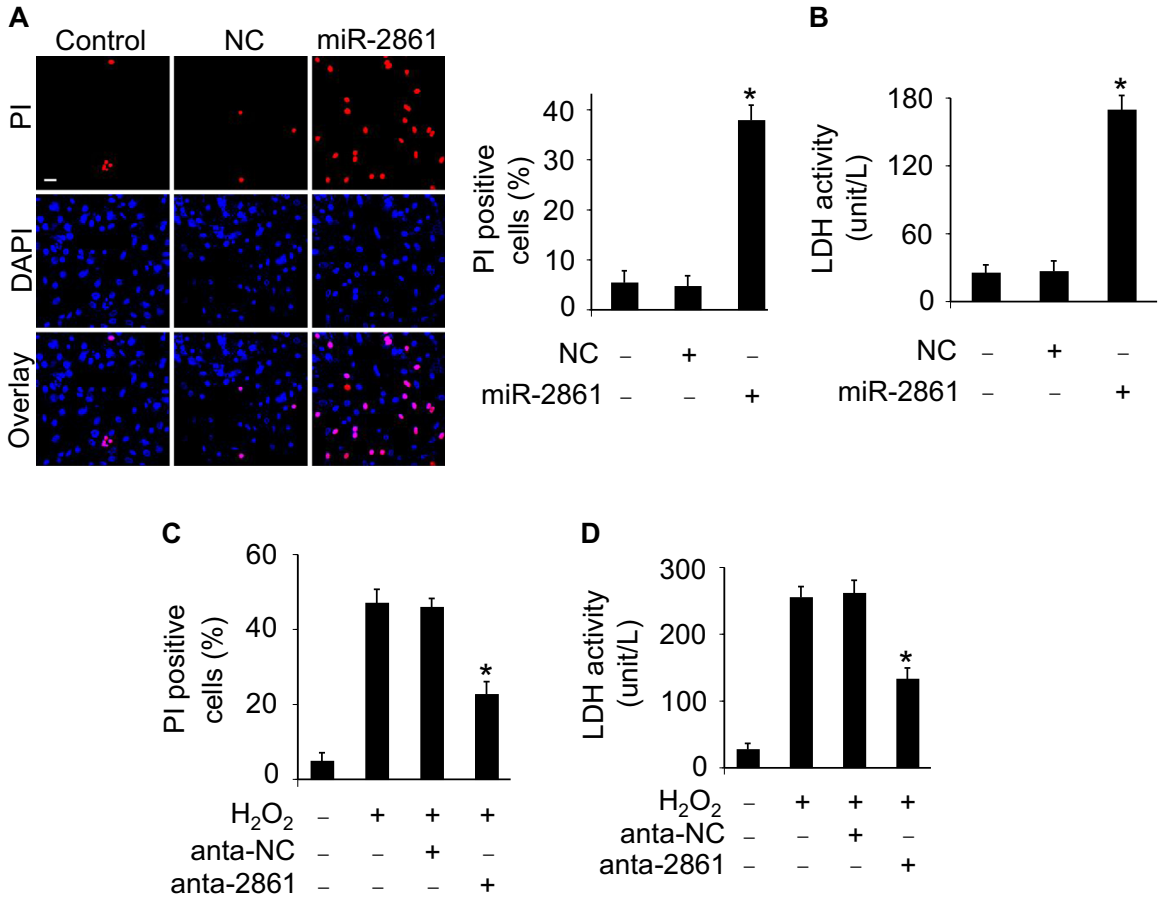

Fig. 4. miR-2861 promotes necrosis in cardiomyocytes. (A) Cardiomyocytes were transfected with mimic miR-2861 or mimic control (NC). 48 h after transfection necrosis was assessed by PI exclusion. Representative images showed PI-positive cells (left panel). Bar = 20 μm. The quantitative analysis of necrosis was shown in (right panel). $^{*}p < 0.05$ vs control. (B) Cardiomyocytes were treated as described in (A), LDH activity was measured. $^{*}p < 0.05$ vs control. (C and D) Knockdown of miR-2861 reduces necrotic responses induced by H_2O_2. Cardiomyocytes were transfected with anta-2861 or anta-NC. 24 h after transfection cells were treated with H_2O_2. Necrosis was assessed by PI exclusion (C) and LDH activity (D). $^{*}p < 0.05$ vs H_2O_2 alone.

Fig. 4B). And also, ANT1 target protector attenuated I/R-induced myocardial necrosis (Supplementary Fig. 4C). These data suggest that miR-2861 and ANT1 are functionally linked in vitro and in vivo.

Mitochondrial dysfunction is one of the major events responsible for activation of cardiomyocyte cell death pathways during I/R injury. ANT plays an essential role in cellular energy metabolism and provides a continuous supply of ADP to mitochondria [9,10]. Thus, we explored the role of miR-2861 in mitochondrial function. Given the central role of mitochondria in generating ATP via the electron-transport chain (ETC), we first tested whether miR-2861 altered basal ATP levels. The results showed that miR-2861 knockdown markedly increased ATP levels upon H_2O_2 treatment (Supplementary Fig. 5A). We further determined if miR-2861 knockdown protected mitochondrial respiratory enzyme activities in cardiomyocytes subjected to H_2O_2. As indicated in Supplementary Fig. 5B, miR-2861 knockdown inhibited H_2O_2-induced decrease in complex II activity. Analysis of cardiomyocyte respiratory complex IV activity also shows a similar trend of miR-2861 knockdown mediated protection against H_2O_2 inhibition (Supplementary Fig. 5C). These data suggest that miR-2861 targets ANT1, and mediates mitochondrial functional activities in the cascades of necrotic program.

4. Discussion

In the past, necrosis was considered to be a passive and unregulated cell death event which is characterized by cell membrane rupture and organelle swelling. Recently, studies have demonstrated that necrosis can be executed by a tightly regulated signaling and is termed programmed necrosis or necroptosis [29–31]. Programmed necrosis has been found to participate in the regulation of physiological and pathological process. It was reported that RIP3 controls programmed necrosis and is necessary for the inflammatory response against virus infections [32]. In addition, programmed necrosis is also involved in the tissue damage disease [31]. Particularly, necrosis is also involved in the pathogenesis of heart disease [33]. Signaling through death receptor and mitochondrial pathway all can lead to programmed necrosis in the heart with activation of RIP kinase [31,34]. Consistent with previous studies, data from this study further supported programmed necrosis could be regulated in the heart. Our present work demonstrated that miR-2861 regulates programmed necrosis through targeting ANT1 in the heart. Knockdown of miR-2861 inhibited cardiomyocyte necrosis and reduced myocardial infarction. Our study reveals a novel molecular mechanism of myocardial necrosis and provides the therapeutic targets for treating myocardial infarction and heart failure.

Several previous studies suggest that ANT1 might have important functions in the heart which remains an enigma. ANT1 was ubiquitinated in mouse heart [35]. Large scale analysis and mass spectrometry revealed that lysine succinylation of ANT1 was involved in mitochondrial metabolism [36]. ANT1 (−/−) mice have biochemical, histological, metabolic and physiological characteristics of mitochondrial myopathy and cardiomyopathy [37].

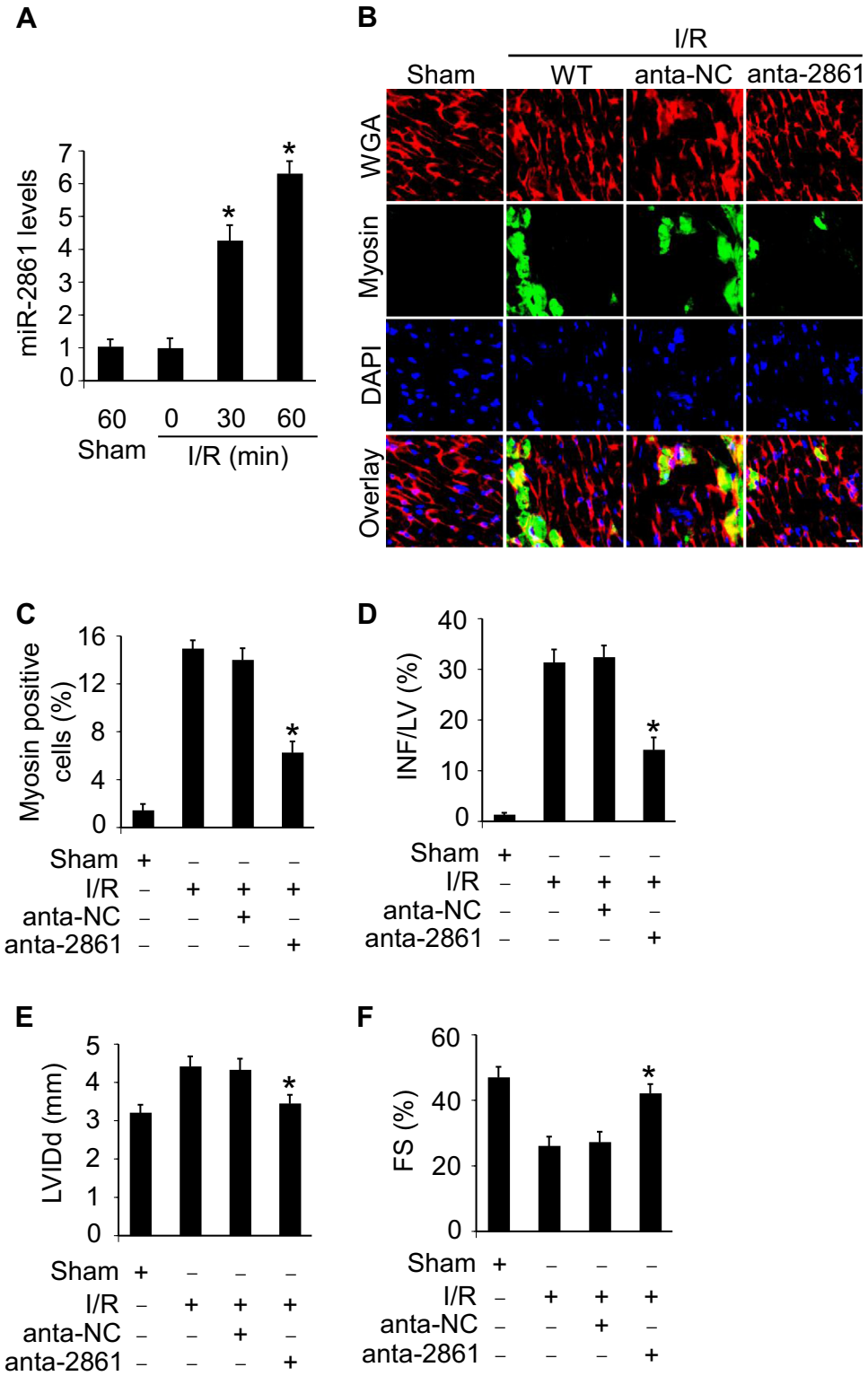

Fig. 5. Knockdown of miR-2861 inhibits necrotic cell death in the heart. (A) miR-2861 levels during myocardial ischemia/reperfusion (I/R). Mice were subjected to cardiac I/R at the indicated time. Sham-operated group served as negative control. Ischemic zone were prepared at the indicated time for qRT-PCR analysis of miR-2861 levels ($n=6$). $^{*}p<0.05$ vs 0 min or sham. (B and C) Knockdown of miR-2861 attenuates myocardial necrosis upon I/R injury. In vivo delivery of anta-2861 or anta-NC was performed as described in Methods. The mice were subjected to sham or I/R as described in the Methods. Myosin antibody was injected into the mice to label necrotic cells. Representative images of ventricular myocardium sections from sham operation or I/R are shown in (B) and the quantitative analysis of myosin positive cells is shown in (C). $n=6$. Green, immunohistochemistry for myosin antibody incorporation into the heart; Red, wheat germ stain for cell membranes; Blue, DAPI-stained nuclei. Bar=20 μm. $^{*}p<0.05$ vs I/R alone. (D) Knockdown of miR-2861 attenuates myocardial infarction sizes. Mice were treated as described in (C). Myocardial infarct sizes were measured as described in Methods. Infarct size was shown. Left ventricle (LV), infarct area (INF) ($n=6$). $^{*}p<0.05$ vs I/R alone. (E and F) Left ventricular dimensions and cardiac function in mice exposed to I/R were analyzed. Mice were treated as described in (C). Transthoracic echocardiographic analysis was performed after 60 min ischemia followed by 1 week reperfusion. LVIDd, diastolic left ventricular internal diameters; FS, fractional shortening of left ventricular diameter, calculated as $[(\text{LVIDd}-\text{LVIDs})/\text{LVIDd}]\times 100$ ($n=6$). $^{*}p<0.05$ vs I/R alone. (For interpretation of the references to color in this figure legend, the reader is referred to the web version of this article.)

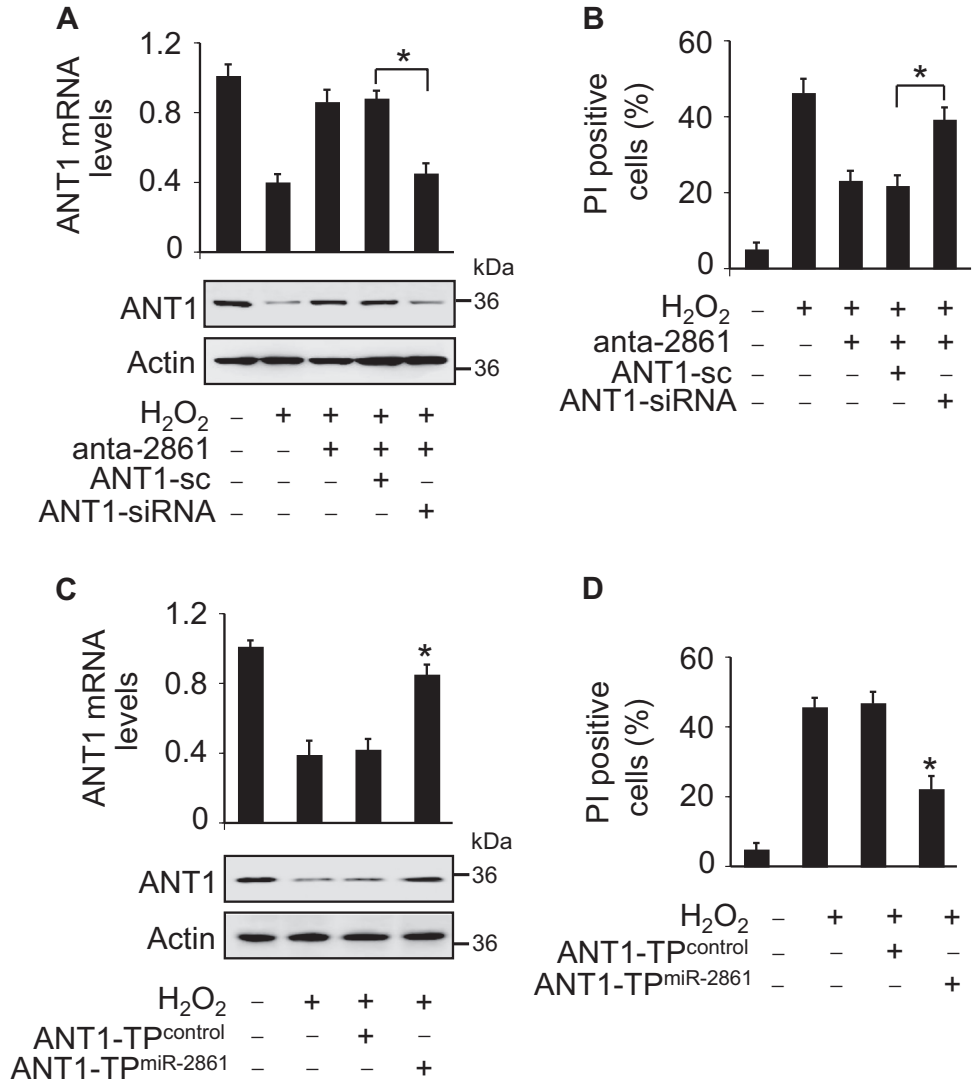

Fig. 6. miR-2861 regulates necrosis through ANT1. (A and B) Knockdown of ANT1 attenuates the effect of miR-2861 knockdown on ANT1 expression and necrotic cell death induced by H_2O_2. Cardiomyocytes were infected with adenoviral ANT1-siRNA, ANT1-sc, transfected with anta-2861, 24 h after transfection cells were exposed to 700 μM H_2O_2 for 24 h. The mRNA and protein levels were analyzed by qRT-PCR (A, upper panel) and immunoblot (A, low panel). $n=4$. Necrotic cells were analyzed by PI assay (B). $n=4$. $^*p<0.05$. (C and D) ANT1 target protector reduces the effect of H_2O_2 on ANP1 expression and necrosis. Cardiomyocytes were transfected with the target protector ($ANP1\text{-}TP^{miR\text{-}2861}$) or the control ($ANP1\text{-}TP^{control}$), and then were exposed to 700 μM H_2O_2 for 24 h. ANP1 expression levels were analyzed by qRT-PCR (C, upper panel) and immunoblot (C, low panel). Necrotic cell death was assessed by PI exclusion assay (D). $^*p<0.05$ vs H_2O_2 alone.

These studies suggest that ANT1 might play an essential role in the heart. Here, our studies for the first time identified that ANT1 participated in the regulation of H_2O_2- or I/R-induced myocardial necrosis. The discovery of ANT1 in necrotic cell death may shed new light on understanding the complex molecular mechanisms of cardiac infarction.

Although the function of miRNAs has been widely studied in cardiomyocytes and animal models of heart failure, the mechanism of miRNAs in cardiomyocytes necrosis remains largely unknown. Previous study shows that miR-2861 targeting HDAC5 and regulates osteoblast differentiation in mice [38]. And miR-2861 functions in osteoblast differentiation by a novel Runx2/miR-3960/miR-2861 regulatory feedback loop [39]. The role of miR-2861 in the heart remains unidentified. Our data showed that miR-2861 was upregulated in cardiomyocytes exposed to H_2O_2 and in I/R heart. The present study firstly demonstrated that miR-2861 participated in the regulation of necrosis and myocardial infarction through targeting ANT1. Knockdown of miR-2861 significantly attenuated necrosis in the cellular model and reduced the myocardial infarction size in the animal model upon I/R injury. Our study has provided important evidences about the function of microRNAs in the programmed necrosis pathway, a step toward better understanding the miRNA-based therapy for I/R injury and heart failure. Whether miR-2861 are involved in the regulation of necrosis in other tissues or cell types such as cancer is an interesting question for future investigation.

Usually, miRNAs translationally inhibit mRNA by binding to the 3′-untranslated regions (3′-UTR). Hitherto, several reports demonstrate that miRNAs that bind to the coding region (CDS) of mRNA have the potential to repress the translation or promote degradation of the mRNA [40]. For example, miR-148 represses DNA methyltransferase 3b (Dnmt3b) gene expression through a region in its coding sequence [41]. miR-183 regulates βTrCP1 levels and activity by targeting to the coding region of βTrCP1 mRNA and triggering mRNA degradation [42]. Consistent with these reports, our results revealed that miR-2861 has specific binding sites on ANT1 CDS. Our study for the first time suggests that miR-2861 inhibits the function of ANT1 by binding to the CDS rather than the 3′UTR. This result greatly expands the functional network of miRNA in the heart. Also, our studies provide new insights in

understanding the cellular and molecular mechanisms that underlie the onset of heart diseases.

Funding sources

This work was supported by National Natural Science Foundation of China (81270160, 81470522, and 81522005), Beijing Municipal Natural Science Foundation (7142103).

Conflict of interest

The authors declare no conflict of interest.

Appendix A. Supplementary material

Supplementary data associated with this article can be found in the online version at http://dx.doi.org/10.1016/j.freeradbiomed.2015.11.031.

References

[1] G. Olivetti, R. Abbi, F. Quaini, J. Kajstura, W. Cheng, J.A. Nitahara, E. Quaini, C. Di Loreto, C.A. Beltrami, S. Krajewski, J.C. Reed, P. Anversa, Apoptosis in the failing human heart, N. Engl. J. Med. 336 (1997) 1131–1141.
[2] L. Hofstra, H. Liem, E.A. Dumont, H.H. Boersma, W.L. van Heerde, P. A. Doevendans, E. DeMuinck, H. Wellens, G.J. Kemerink, C.P. Reutelingsperger, Visualisation of cell death in vivo in patients with acute myocardial infarction, Lancet 356 (2000) 209–212.
[3] J.X. Wang, X. Zhang, Q. Li, K. Wang, Y. Wang, J. Jiao, C. Feng, S. Teng, L.Y. Zhou, Y. Gong, Z. Zhou, J. Liu, J.L. Wang, P. Li, Microrna-103/107 regulate programmed necrosis and myocardial ischemia/reperfusion injury through targeting fadd, Circ. Res. (2015).
[4] K. Wang, F. Liu, L.Y. Zhou, S.L. Ding, B. Long, C.Y. Liu, T. Sun, Y.Y. Fan, L. Sun, P. F. Li, Mir-874 regulates myocardial necrosis by targeting caspase-8, Cell Death Dis. 4 (2013) e709.
[5] B.A. Ballif, G.R. Carey, S.R. Sunyaev, S.P. Gygi, Large-scale identification and evolution indexing of tyrosine phosphorylation sites from murine brain, J. Proteom. Res. 7 (2008) 311–318.
[6] J.W. Ellison, X. Li, U. Francke, L.J. Shapiro, Rapid evolution of human pseudoautosomal genes and their mouse homologs, Mamm. Genome: Off. J. Int. Mamm. Genome Soc. 7 (1996) 25–30.
[7] J.D. Sharer, J.F. Shern, H. Van Valkenburgh, D.C. Wallace, R.A. Kahn, Arl2 and bart enter mitochondria and bind the adenine nucleotide transporter, Mol. Biol. Cell 13 (2002) 71–83.
[8] C. Fiore, V. Trezeguet, A. Le Saux, P. Roux, C. Schwimmer, A.C. Dianoux, F. Noel, G.J. Lauquin, G. Brandolin, P.V. Vignais, The mitochondrial adp/atp carrier: structural, physiological and pathological aspects, Biochimie 80 (1998) 137–150.
[9] A.K. Carroll, W.R. Clevenger, T. Szabo, L.E. Ackermann, Y. Pei, S.S. Ghosh, S. Glasco, R. Nazarbaghi, R.E. Davis, C.M. Anderson, Ectopic expression of the human adenine nucleotide translocase, isoform 3 (ant-3). Characterization of ligand binding properties, Mitochondrion 5 (2005) 1–13.
[10] T. Walther, C. Tschöpe, A. Sterner-Kock, D. Westermann, S. Heringer-Walther, A. Riad, A. Nikolic, Y. Wang, L. Ebermann, W.-E. Siems, Accelerated mitochondrial adenosine diphosphate/adenosine triphosphate transport improves hypertension-induced heart disease, Circulation 115 (2007) 333–344.
[11] M.A. Portman, Y. Xiao, K. Qian, R.L. Tucker, S.M. Parish, X.H. Ning, Thyroid hormone coordinates respiratory control maturation and adenine nucleotide translocator expression in heart in vivo, Circulation 102 (2000) 1323–1329.
[12] R.C. Lee, R.L. Feinbaum, V. Ambros, The *C. elegans* heterochronic gene lin-4 encodes small rnas with antisense complementarity to lin-14, Cell 75 (1993) 843–854.
[13] B.J. Reinhart, F.J. Slack, M. Basson, A.E. Pasquinelli, J.C. Bettinger, A.E. Rougvie, H.R. Horvitz, G. Ruvkun, The 21-nucleotide let-7 rna regulates developmental timing in *Caenorhabditis elegans*, Nature 403 (2000) 901–906.
[14] L. Qian, L.W. Van Laake, Y. Huang, S. Liu, M.F. Wendland, D. Srivastava, Mir-24 inhibits apoptosis and represses bim in mouse cardiomyocytes, J. Exp. Med. 208 (2011) 549–560.
[15] X. Wang, X. Zhang, X.P. Ren, J. Chen, H. Liu, J. Yang, M. Medvedovic, Z. Hu, G. C. Fan, Microrna-494 targeting both proapoptotic and antiapoptotic proteins protects against ischemia/reperfusion-induced cardiac injury, Circulation 122 (2010) 1308–1318.
[16] D. Sayed, M. He, C. Hong, S. Gao, S. Rane, Z. Yang, M. Abdellatif, Microrna-21 is a downstream effector of akt that mediates its antiapoptotic effects via suppression of fas ligand, J. Biol. Chem. 285 (2010) 20281–20290.
[17] P. Li, Microrna in cardiac apoptosis, J. Cardiovasc. Transl. Res. 3 (2010) 219–224.
[18] M. Basson, Microrna loom large in the heart, Nat. Med. 13 (2007) 541.
[19] Y. Zhao, J.F. Ransom, A. Li, V. Vedantham, M. von Drehle, A.N. Muth, T. Tsuchihashi, M.T. McManus, R.J. Schwartz, D. Srivastava, Dysregulation of cardiogenesis, cardiac conduction, and cell cycle in mice lacking mirna-1-2, Cell 129 (2007) 303–317.
[20] B. Yang, H. Lin, J. Xiao, Y. Lu, X. Luo, B. Li, Y. Zhang, C. Xu, Y. Bai, H. Wang, G. Chen, Z. Wang, The muscle-specific microrna mir-1 regulates cardiac arrhythmogenic potential by targeting gja1 and kcnj2, Nat. Med. 13 (2007) 486–491.
[21] T. Thum, P. Galuppo, C. Wolf, J. Fiedler, S. Kneitz, L.W. van Laake, P. A. Doevendans, C.L. Mummery, J. Borlak, A. Haverich, C. Gross, S. Engelhardt, G. Ertl, J. Bauersachs, Microrna in the human heart: a clue to fetal gene reprogramming in heart failure, Circulation 116 (2007) 258–267.
[22] K.R. Chien, Molecular medicine: micrornas and the tell-tale heart, Nature 447 (2007) 389–390.
[23] W.Q. Tan, K. Wang, D.Y. Lv, P.F. Li, Foxo3a inhibits cardiomyocyte hypertrophy through transactivating catalase, J. Biol. Chem. 283 (2008) 29730–29739.
[24] Z. Lin, I. Murtaza, K. Wang, J. Jiao, J. Gao, P.F. Li, Mir-23a functions downstream of nfatc3 to regulate cardiac hypertrophy, Proc. Natl. Acad. Sci. USA 106 (2009) 12103–12108.
[25] C. Chen, D.A. Ridzon, A.J. Broomer, Z. Zhou, D.H. Lee, J.T. Nguyen, M. Barbisin, N.L. Xu, V.R. Mahuvakar, M.R. Andersen, K.Q. Lao, K.J. Livak, K.J. Guegler, Real-time quantification of microrna by stem-loop rt-pcr, Nucleic Acids Res. 33 (2005) e179.
[26] P.F. Li, R. Dietz, R. von Harsdorf, P53 regulates mitochondrial membrane potential through reactive oxygen species and induces cytochrome c-independent apoptosis blocked by bcl-2, Embo J. 18 (1999) 6027–6036.
[27] I. Murtaza, H.X. Wang, X. Feng, N. Alenina, M. Bader, B.S. Prabhakar, P.F. Li, Down-regulation of catalase and oxidative modification of protein kinase ck2 lead to the failure of apoptosis repressor with caspase recruitment domain to inhibit cardiomyocyte hypertrophy, J. Biol. Chem. 283 (2008) 5996–6004.
[28] J.X. Wang, J.Q. Jiao, Q. Li, B. Long, K. Wang, J.P. Liu, Y.R. Li, P.F. Li, Mir-499 regulates mitochondrial dynamics by targeting calcineurin and dynamin-related protein-1, Nat. Med. 17 (2011) 71–78.
[29] L. Galluzzi, G. Kroemer, Necroptosis: a specialized pathway of programmed necrosis, Cell 135 (2008) 1161–1163.
[30] K. Moriwaki, F.K. Chan, Rip3: a molecular switch for necrosis and inflammation, Genes Dev. 27 (2013) 1640–1649.
[31] L. Sun, X. Wang, A new kind of cell suicide: mechanisms and functions of programmed necrosis, Trends Biochem. Sci. 39 (2014) 587–593.
[32] Y.S. Cho, S. Challa, D. Moquin, R. Genga, T.D. Ray, M. Guildford, F.K. Chan, Phosphorylation-driven assembly of the rip1–rip3 complex regulates programmed necrosis and virus-induced inflammation, Cell 137 (2009) 1112–1123.
[33] M. Luedde, M. Lutz, N. Carter, J. Sosna, C. Jacoby, M. Vucur, J. Gautheron, C. Roderburg, N. Borg, F. Reisinger, H.J. Hippe, A. Linkermann, M.J. Wolf, S. Rose-John, R. Lullmann-Rauch, D. Adam, U. Flogel, M. Heikenwalder, T. Luedde, N. Frey, Rip3, a kinase promoting necroptotic cell death, mediates adverse remodelling after myocardial infarction, Cardiovasc. Res. 103 (2014) 206–216.
[34] G. Kung, K. Konstantinidis, R.N. Kitsis, Programmed necrosis, not apoptosis, in the heart, Circ. Res. 108 (2011) 1017–1036.
[35] H.B. Jeon, E.S. Choi, J.H. Yoon, J.H. Hwang, J.W. Chang, E.K. Lee, H.W. Choi, Z. Y. Park, Y.J. Yoo, A proteomics approach to identify the ubiquitinated proteins in mouse heart, Biochem. Biophys. Res. Commun. 357 (2007) 731–736.
[36] J. Park, Y. Chen, D.X. Tishkoff, C. Peng, M. Tan, L. Dai, Z. Xie, Y. Zhang, B. M. Zwaans, M.E. Skinner, D.B. Lombard, Y. Zhao, Sirt5-mediated lysine desuccinylation impacts diverse metabolic pathways, Mol. Cell 50 (2013) 919–930.
[37] B.H. Graham, K.G. Waymire, B. Cottrell, I.A. Trounce, G.R. MacGregor, D. C. Wallace, A mouse model for mitochondrial myopathy and cardiomyopathy resulting from a deficiency in the heart/muscle isoform of the adenine nucleotide translocator, Nat. Genet. 16 (1997) 226–234.
[38] S. Fischer, A.J. Paul, A. Wagner, S. Mathias, M. Geiss, F. Schandock, M. Domnowski, J. Zimmermann, R. Handrick, F. Hesse. Mir-2861 as novel hdac5 inhibitor in cho cells enhances productivity while maintaining product quality. Biotechnol. Bioeng., 2015.
[39] R. Hu, W. Liu, H. Li, L. Yang, C. Chen, Z.-Y. Xia, L.-J. Guo, H. Xie, H.-D. Zhou, X.-P. Wu, A runx2/mir-3960/mir-2861 regulatory feedback loop during mouse osteoblast differentiation, J. Biol. Chem. 286 (2011) 12328–12339.
[40] J. Hausser, A.P. Syed, B. Bilen, M. Zavolan, Analysis of cds-located mirna target sites suggests that they can effectively inhibit translation, Genome Res. 23 (2013) 604–615.
[41] A.M. Duursma, M. Kedde, M. Schrier, C. Le Sage, R. Agami, Mir-148 targets human dnmt3b protein coding region, Rna 14 (2008) 872–877.
[42] I. Elcheva, S. Goswami, F.K. Noubissi, V.S. Spiegelman, Crd-bp protects the coding region of βtrcp1 mrna from mir-183-mediated degradation, Mol. Cell 35 (2009) 240–246.